Designing qubits with Superconducting Circuits

by

Fırat Solğun

A Thesis Submitted to the
Graduate School of Sciences and Engineering
in Partial Fulfillment of the Requirements for
the Degree of

Master of Science

in

Physics

Koç University

10 August 2011

Koç University

Graduate School of Sciences and Engineering

This is to certify that I have examined this copy of a master's thesis by

Fırat Solğun

and have found that it is complete and satisfactory in all respects,
and that any and all revisions required by the final
examining committee have been made.

Committee Members:

_____

Prof. Tekin Dereli (Advisor)

_____

Assoc. Prof. Özgür Müstecaplıoğlu

_____

Assoc. Prof. Alper Demir

Date: _____

ABSTRACT

We start by reviewing methods to derive hamiltonians for superconducting circuits. By canonical quantization we obtain quantum mechanical description of electrical circuits in the low temperature limit. We then look at some basic superconducting qubit circuits. Some schemes for tunable coupling of qubits to transmission lines are analyzed. We also propose a way to protect qubits during measurement using frequency modulation (FM).

ÖZETÇE

Bu tezde önce süperiletken devrelerin Hamilton operatörlerini bulma yöntemlerini inceliyoruz. Kanonik kuantizasyon yöntemi ile süperiletken devrelerin düşük sıcaklık limitindeki kuantum mekaniksel modellerini elde ediyoruz. Daha sonra bazı temel süperiletken kübit devrelerine bakıyoruz. Ardından kübitlerin iletim hatlarına ayarlanabilir şekilde bağlanması için önerilmiş birkaç yöntemi inceliyoruz. Son olarak kübitlerin ölçüm sırasında frekans modülasyonu (FM) ile korunması şeklinde yeni bir yöntem öneriyoruz.

ACKNOWLEDGMENTS

I thank my advisor Tekin Dereli for giving me freedom to work on whatever interested me and for his willingless and patience to listen me; my jury members Özgür Müstecaplıoğlu and Alper Demir for helpful discussions; my friend Omid Khosravani for thinking about my questions even he had some other important things to do.

I thank TUBITAK for their financial support through 2210 fellowship program.

I thank Michel Devoret for putting his wonderful lectures on the web which I benefited greatly from.

Finally I thank my family for their support.

TABLE OF CONTENTS

LIST OF FIGURES

Chapter 1

INTRODUCTION

Let us start from the beginning, the Schrödinger equation reads:

$$i\hbar\frac{\partial\psi}{\partial t} = -\frac{\hbar^2}{2m}\nabla^2\psi + U(\vec{r})\,\psi \tag{1.1}$$

The solution $\psi(\vec{r},t)$ under some initial condition is called the *wavefunction* and $|\psi(\vec{r},t)|^2 d\vec{r}$ gives the probability of finding the particle at position $\vec{r}$ at time t. Now one may ask which particle? Usually the particle is an electron orbiting the nucleus of an atom and $U(\vec{r})$ will be the electrostatic potential energy in this case. An interesting question one might ask at this point is whether the Schrödinger equation applies to systems other than atomic particles, to systems of macroscopic size perhaps? But the motion of macroscopic bodies is described by Newton's laws. So is our search for a macroscopic object obeying Schrödinger's equation hopeless? Perhaps not. Think about de Broglie's relation $\lambda = h/p$ which assigns a wave of wavelength λ to every object with momentum p where $h = 6.6262 \times 10^{-34} J \cdot s$ is the Planck's constant. So one can be optimistic and look for macroscopic systems with momenta which will make the wavelength comparable with the dimensions of the system so that quantum behavior will be observable. Note that for a Rydberg atom $\lambda_e = \alpha a_0$ where λ_e is the wavelength of the electron orbiting the nucleus, a_0 the Bohr radius and $\alpha = 1/137$ the fine structure constant.

In fact people have already found systems displaying quantum properties at macroscopic scales. One such system is the so called "RF SQUID" whose circuit diagram is depicted in Figure 1.1 on page 3. The circuit is a superconducting loop of induc-

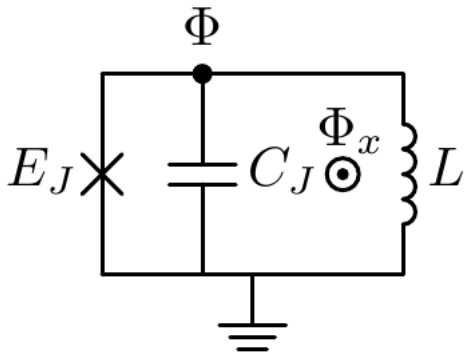

Figure 1.1: RF SQUID

tance L closed in a Josephson junction. The potential energy of the system has a double-well form as a function of the flux across the junction (see Figure 3.5 on page 19). Ground state of each well correspond to the currents flowing in the loop and two lowest eigenstates of the composite system correspond to symmetric and anti-symmetric superpositions of ground states of isolated wells. In this system, the flux $\hat{\Phi}$ across the junction and the charge $\hat{Q}$ on junction's capacitance are conjugate variables in a quantum mechanical sense and satisfy $\left[\hat{\Phi}, \hat{Q}\right] = i\hbar$. Noting that the flux $\hat{\Phi}$ is the variable corresponding to the position operator and the charge $\hat{Q}$ corresponds to momentum operator we can apply the same analysis in the paragraph above. In this case if one assumes that $\hat{Q} \sim 2e$ then the flux wavelength λ_Φ will be of the order of $h/2e = \Phi_0 = 2.0679 \times 10^{-15} T \cdot m^2$, the flux quantum. In the above circuit $\Phi_x \simeq \Phi_0/2$ and $\hat{\Phi} \sim \Phi_0$ is satisfied. RF SQUID display quantum mechanical properties such as quantum tunneling and discrete energy levels which are well verified experimentally.

Our analysis above using de Broglie wavelength sets some range for quantum behaviour. Such an analysis would be enough for closed quantum systems. However open quantum systems interact with their environment which result in irreversible loss of energy and information. Decoherence is the general name given to such processes and it prevents physical realization of quantum computers.

In Chapter 2 we start by reviewing methods to derive hamiltonians for superconducting circuits. In Chapter 3 we look at basic superconducting qubits. Chapter 4 is about tunable coupling of qubits to transmission lines. In Chapter 5 we propose a method to protect qubits against decoherence during measurement with frequency modulation (FM).

Chapter 2

QUANTIZATION OF ELECTRICAL CIRCUITS

2.1 Quantization of lumped element circuits

Electrical engineers have a couple of techniques to solve electrical circuits. They apply node analysis or mesh analysis methods to solve for voltages and currents.

In node analysis method, you choose a reference node which you call as ground and assign a variable e_n to every other node n which represents the voltage at that node. You then write Kirchhoff's voltage and current laws in terms of these node variables and solve them. The voltage difference v_{ab} across the branch between nodes a and b is simply $v_{ab} = e_a - e_b$ and the current through this branch is $i_{ab} = g\left(v_{ab}\right)$ where the conductance function g represents the constitutive relation for that branch.

In mesh analysis you choose independent loops of the circuit and assign loop current variables to each of them. You then write Kirchhoff's laws in terms of these variables. After solving the equations you obtain loop currents and you can write branch currents as a sum of the corresponding loop currents keeping track of the current directions. Branch voltages are obtained by constitutive relations.

Here our aim will be to present a general method to obtain an hamiltonian for a given electrical circuit in terms of independent canonically conjugate variables . We will then apply canonical quantization to these variables and obtain the quantum description of the circuit. Our approach will be based on node analysis [2, 3, 10]. For an approach based on mesh analysis you might consult [8].

The state of each two-terminal device in an electrical circuit is determined by the

voltage across the branch and the current flowing through the device. However a set of branch currents and voltages won't be independent in general since they will be related to each other by Kirchhoff's laws.

To find degrees of freedom of an electrical circuit, we start by defining branch fluxes Φ_b and charges Q_b:

$$\Phi_b(t) = \int_{-\infty}^{t} v(t')\,dt' \tag{2.1}$$

$$Q_b(t) = \int_{-\infty}^{t} i(t')\,dt' \tag{2.2}$$

where $v(t)$ and $i(t)$ are branch voltage and current at time t. We then choose one node of the circuit as ground and construct a spanning tree of the network with respect to this ground node. We can now define node fluxes in terms of the branch fluxes. The flux Φ_i of the node i in the spanning tree is defined as the sum of the branch fluxes over the path joining the ground to that node. One should subtract the branch flux if the path traverses it in the opposite direction.

We can now write the sum of the energies of capacitive elements as a function of derivatives of node fluxes. We call this energy K and consider it as the kinetic energy of the system. Similarly we can get the sum of energies of inductive branches as a function of node fluxes. We call this energy U and associate it with the potential energy of the system. The Lagrangian of the circuit is simply obtained from:

$$\mathcal{L} = K - U \tag{2.3}$$

We define the node charge Q_i as the conjugate momentum Q_i of the node flux Φ_i :

$$Q_i = \frac{\partial \mathcal{L}}{\partial\left(\frac{d\Phi_i}{dt}\right)} \tag{2.4}$$

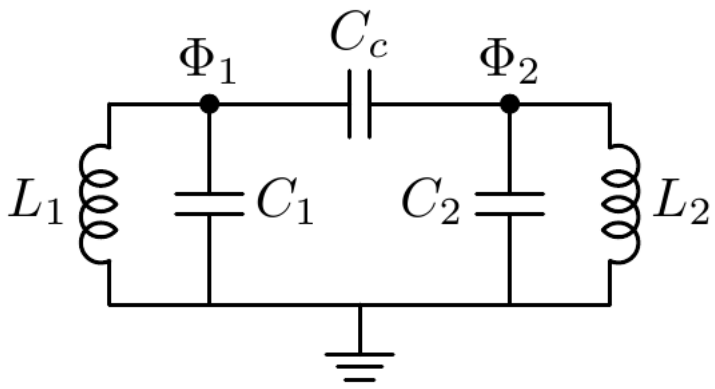

Figure 2.1: Coupled oscillators

The quantity Q_i is equal to the sum of the charges stored in the plates of the capacitors connected to the node i . The Poisson bracket of these conjugate variables is unity:

$$\{\Phi, Q\} = 1 \tag{2.5}$$

We write the hamiltonian directly as the sum of kinetic and potential energies:

$$\mathcal{H} = K + U \tag{2.6}$$

We can now apply canonical quantization procedure by simply replacing classical variables by their quantum equivalents:

$$\Phi \leftarrow \hat{\Phi} \tag{2.7}$$

$$Q \leftarrow \hat{Q} \tag{2.8}$$

$$\mathcal{H} \leftarrow \hat{\mathcal{H}} \tag{2.9}$$

Let's demonstrate the quantization procedure by working out the circuit in Figure 2.1 on page 7.

The circuit has two nodes with node fluxes Φ_1 and Φ_2 connected to ground over LC circuits and connected to each other over a coupling capacitor C_c . The reduced capacitance matrix for these nodes reads [6]:

$$C_r = \begin{bmatrix} C_1 + C_c & -C_c \\ -C_c & C_2 + C_c \end{bmatrix} \tag{2.10}$$

The kinetic energy K is the electrostatic energy stored in the circuit and given by:

$$K = \frac{1}{2} Q^T C_r^{-1} Q \tag{2.11}$$

$$= \frac{Q_1^2}{2C_1'} + \frac{Q_1 Q_2}{2C_c'} + \frac{Q_2^2}{2C_2'} \tag{2.12}$$

where

$$C_1' = \frac{C_1 C_2 + C_c (C_1 + C_2)}{C_2 + C_c} \tag{2.13}$$

$$C_2' = \frac{C_1 C_2 + C_c (C_1 + C_2)}{C_1 + C_c} \tag{2.14}$$

$$C_c' = \frac{C_1 C_2 + C_c (C_1 + C_2)}{2C_c} \tag{2.15}$$

The potential energy U is the magnetic energy stored in the inductors:

$$U = \frac{\Phi_1^2}{2L_1} + \frac{\Phi_2^2}{2L_2} \tag{2.16}$$

So that the quantum hamiltonian is:

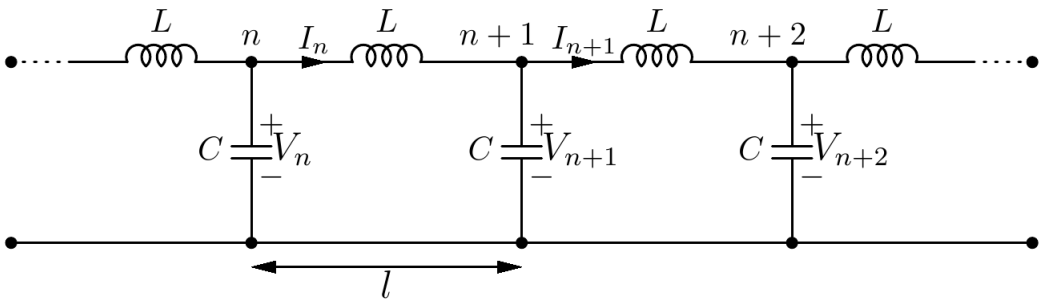

Figure 2.2: LC ladder model of a transmission line

$$\hat{H} = \hat{K} + \hat{U} \tag{2.17}$$

$$= \frac{\hat{Q}_1^2}{2C_1'} + \frac{\hat{Q}_1\hat{Q}_2}{2C_c'} + \frac{\hat{Q}_2^2}{2C_2'} + \frac{\hat{\Phi}_1^2}{2L_1} + \frac{\hat{\Phi}_2^2}{2L_2} \tag{2.18}$$

2.2 Quantization of transmission lines

Transmission line is not a lumped circuit element but rather a distributed medium. A model for a transmission line is presented in Figure 2.2 on page 9. In this model equations for currents and voltages read:

$$V_n - V_{n+1} = L\frac{d}{dt}I_n \tag{2.19}$$

$$I_{n-1} - I_n = C\frac{d}{dt}V_n \tag{2.20}$$

Dividing both sides of the above equations by the length of a cell in the LC ladder and taking the $l \to 0$ limit we get:

$$\frac{\partial V}{\partial x} = -L_l \frac{\partial I}{\partial t} \tag{2.21}$$

$$\frac{\partial I}{\partial x} = -C_l \frac{\partial V}{\partial t} \tag{2.22}$$

where L_l and C_l are the inductance and capacitance per unit length. Introducing left and right propagating wave amplitudes $A^{\leftarrow}$ and $A^{\rightarrow}$:

$$V(x,t) = V^{\rightarrow} + V^{\leftarrow} = \sqrt{Z_c}\left(A^{\rightarrow}(x,t) + A^{\leftarrow}(x,t)\right) \tag{2.23}$$

$$I(x,t) = I^{\rightarrow} - I^{\leftarrow} = \frac{1}{\sqrt{Z_c}}\left(A^{\rightarrow}(x,t) - A^{\leftarrow}(x,t)\right) \tag{2.24}$$

where $Z_c = \sqrt{\frac{L_l}{C_l}}$ is the characteristic impedance of the line, the Telegrapher's equations Eq. (2.21) and Eq. (2.22) become:

$$\frac{\partial}{\partial x} A^{\rightarrow} = -\frac{1}{v_p}\frac{\partial}{\partial t} A^{\rightarrow} \tag{2.25}$$

$$\frac{\partial}{\partial x} A^{\leftarrow} = \frac{1}{v_p}\frac{\partial}{\partial t} A^{\leftarrow} \tag{2.26}$$

where $v_p = \frac{1}{\sqrt{L_l C_l}}$ is the propagation velocity. Equations (2.25) and (2.26) has solutions:

$$A^{\rightarrow}(x,t) = A_0^{\rightarrow}(x - v_p t) \tag{2.27}$$

$$A^{\leftarrow}(x,t) = A_0^{\leftarrow}(x + v_p t) \tag{2.28}$$

for some shape functions $A_0^{\rightarrow}$ and $A_0^{\leftarrow}$.

Now let's define the flux $\Phi(x,t)$ at point x on the transmission line as follows:

$$\Phi(x,t) = \int_{-\infty}^{t} d\tau V(x,\tau) \tag{2.29}$$

Lagrangian density reads:

$$\mathcal{L}(x) = \frac{C_l}{2}\left(\frac{\partial\Phi}{\partial t}\right)^2 - \frac{1}{2L_l}\left(\frac{\partial\Phi}{\partial x}\right)^2 \tag{2.30}$$

Momentum conjugate to the flux variable $\Phi(x,t)$ is the charge density $\Pi(x,t)$ on the line:

$$\Pi(x,t) = \frac{\partial\mathcal{L}}{\partial\left(\frac{\partial\Phi}{\partial t}\right)} = C_l V(x,t) \tag{2.31}$$

By canonical quantization, Φ and Π become operators $\hat{\Phi}$ and $\hat{\Pi}$ satisfying:

$$\left[\hat{\Phi}(x_1), \hat{\Pi}(x_2)\right] = i\hbar\delta(x_1 - x_2) \tag{2.32}$$

In this representation hamiltonian reads:

$$\hat{\mathcal{H}} = \int_{-\infty}^{+\infty} dx \left[\frac{1}{2C_l}\left(\hat{\Pi}(x)\right)^2 + \frac{1}{2L_l}\left(\frac{\partial\hat{\Phi}}{\partial x}\right)^2\right] \tag{2.33}$$

We now Fourier transform $\hat{\Phi}$ and $\hat{\Pi}$ to get:

$$\hat{\Phi}[k] = \frac{1}{\sqrt{2\pi}}\int_{-\infty}^{+\infty} dx\hat{\Phi}(x)\, e^{-ikx} \tag{2.34}$$

$$\hat{\Pi}[k] = \frac{1}{\sqrt{2\pi}}\int_{-\infty}^{+\infty} dx\hat{\Pi}(x)\, e^{-ikx} \tag{2.35}$$

with the commutation relation $\left[\hat{\Phi}[k_1], \hat{\Pi}[k_2]\right] = i\hbar\delta(k_1 + k_2)$.

One can introduce field ladder operators $\hat{a}[k]$ and $\hat{a}^\dagger[k]$:

$$\hat{a}[k] = \frac{1}{\sqrt{2\hbar}}\left[\sqrt{\omega(k)C_l}\hat{\Phi}[k] + \frac{i}{\sqrt{\omega(k)C_l}}\hat{\Pi}[k]\right] \tag{2.36}$$

$$\hat{a}^\dagger[k] = \frac{1}{\sqrt{2\hbar}}\left[\sqrt{\omega(k)C_l}\hat{\Phi}[-k] - \frac{i}{\sqrt{\omega(k)C_l}}\hat{\Pi}[-k]\right] \tag{2.37}$$

$\omega(k)$ is given by the dispersion relation $\omega^2(k) = v_p^2 k^2 = \frac{k^2}{C_l L_l}$.

We will now extend ladder operators to negative frequencies for both right and left moving fields as follows [2]:

$$\hat{a}^{\rightarrow}[\omega] = \begin{cases} \hat{a}[\omega] & \omega > 0 \\ \hat{a}^\dagger[-\omega] & \omega < 0 \end{cases} \quad k > 0 \tag{2.38}$$

$$\hat{a}^{\leftarrow}[\omega] = \begin{cases} \hat{a}[\omega] & \omega > 0 \\ \hat{a}^\dagger[-\omega] & \omega < 0 \end{cases} \quad k < 0 \tag{2.39}$$

Now the hamiltonian reads in terms of ladder operators:

$$\hat{\mathcal{H}} = \int_0^\infty \hbar\omega d\omega \left(\hat{a}^{\leftarrow}[-\omega]\hat{a}^{\leftarrow}[\omega] + \hat{a}^{\rightarrow}[-\omega]\hat{a}^{\rightarrow}[\omega]\right) \tag{2.40}$$

with zero-point energy subtracted. Positive frequencies correspond to photon emission whereas negative frequencies correspond to the absorption of a photon.

Note that the frequency variable ω is still continuous and one should construct a countable basis in time and frequency to obtain a discrete frequency index hence photon operators.

Chapter 3

BASIC SUPERCONDUCTING QUBITS

In this section, we will look at some basic superconducting qubits. Depending on the relative strength of charging energy E_C vs Josephson energy E_J , they are called a *charge qubit* or a *flux qubit*. For a charge qubit $E_C \gg E_J$ is true whereas for a flux qubit $E_J \gg E_C$ holds.

3.1 Charge Qubits

3.1.1 The Cooper pair box

The Cooper pair box is the most basic circuit operating in the charging regime $E_C \gg E_J$. It consists of a superconducting island connected to a superconducting reservoir through a josephson junction. The island is biased by a voltage source connected over a gate capacitance, see Figure 3.1 on page 13.

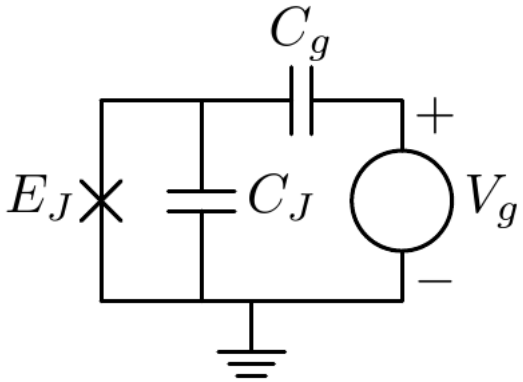

Figure 3.1: The Cooper pair box circuit

We write the electrostatic energy stored in the circuit as:

$$\hat{K} = \frac{1}{2\left(C_J + C_g\right)}\left(\hat{Q} - C_g V_g\right)^2 \tag{3.1}$$

where $\hat{Q}$ is the charge on the island conjugate to the flux $\hat{\Phi}$ across the junction with $\left[\hat{\Phi}, \hat{Q}\right] = i\hbar$.

The potential energy term is the Josephson energy of the junction:

$$\hat{U} = -E_J cos\left(2\pi\hat{\Phi}/\Phi_0\right) \tag{3.2}$$

So that the hamiltonian for the Cooper pair box reads:

$$\hat{H} = \hat{K} + \hat{U} = \frac{1}{2\left(C_J + C_g\right)}\left(\hat{Q} - C_g V_g\right)^2 - E_J cos\left(2\pi\hat{\Phi}/\Phi_0\right) \tag{3.3}$$

One way to solve this hamiltonian is to work in the charge basis $\{|n\rangle\}$ satisfying:

$$\hat{n}\,|n\rangle = n\,|n\rangle \tag{3.4}$$

where the operator $\hat{n}$ represents the number of Cooper pairs tunneled through the junction or the number of excess Cooper pairs on the island. Note that $\hat{n} = \hat{Q}/2e$ and $n \in \mathbb{Z}$. The operator conjugate to $\hat{n}$ is the phase $\hat{\theta}$ of the superconducting island. Note also that since n is discrete the wavefunction in θ space will be periodic with period 2π . Charge and phase states satisfy the usual Fourier transform relations for conjugate variables:

$$|\theta\rangle = \frac{1}{\sqrt{2\pi}}\sum_{n\in\mathbb{Z}} exp\left(in\theta\right)|n\rangle \tag{3.5}$$

$$|n\rangle = \frac{1}{\sqrt{2\pi}}\int_0^{2\pi} d\theta exp\left(-in\theta\right)|\theta\rangle \tag{3.6}$$

which implies the following translation relation:

$$exp\left(ip\hat{\theta}\right)|n\rangle = |n-p\rangle \tag{3.7}$$

$$exp\left(i\theta_0\hat{n}\right)|\theta\rangle = |\theta+\theta_0\rangle \tag{3.8}$$

The superconducting phase $\hat{\theta}$ of the island is related to the flux $\hat{\Phi}$ across the junction by the following relation:

$$\hat{\theta} = 2\pi\hat{\Phi}/\Phi_0 \tag{3.9}$$

So the potential energy term can be written in the charge basis:

$$\hat{U} = -E_J cos\left(2\pi\hat{\Phi}/\Phi_0\right) \tag{3.10}$$

$$= -E_J cos\left(\hat{\theta}\right) \tag{3.11}$$

$$= -E_J\left(e^{i\hat{\theta}} + e^{-i\hat{\theta}}\right)/2 \tag{3.12}$$

$$= -\frac{E_J}{2}\sum_{n\in\mathbb{Z}}\left(|n+1\rangle\langle n| + |n\rangle\langle n+1|\right) \tag{3.13}$$

where in the last step we have used the translation property in Eq. (3.7).

The kinetic energy in the charge basis reads:

$$\hat{K} = E_C\left(\hat{n} - n_g\right)^2 \tag{3.14}$$

where $E_C = \frac{(2e)^2}{C_J+C_g}$ and $n_g = \frac{C_g V_g}{2e}$. The hamiltonian in charge basis now reads:

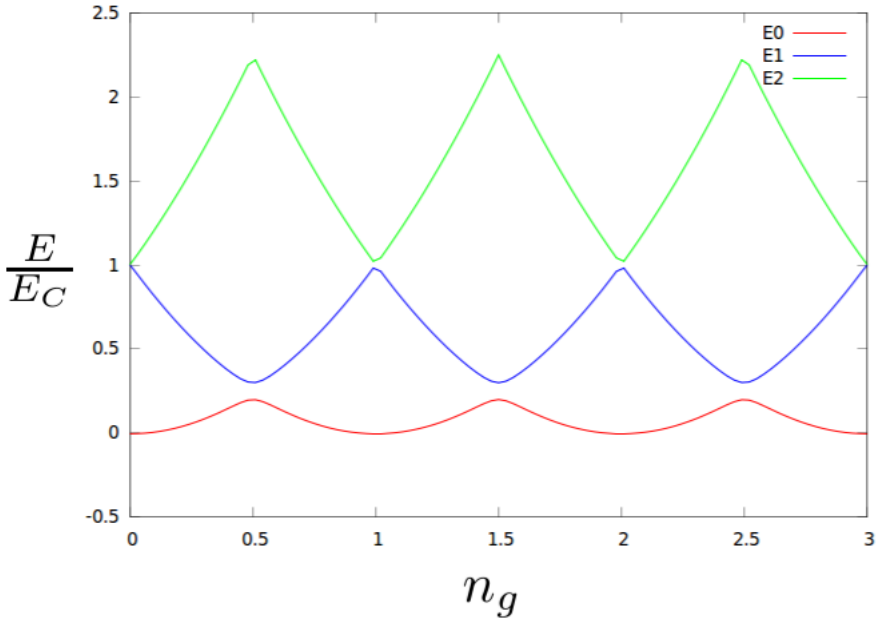

Figure 3.2: Cooper Pair Box energy bands (First 3 energy eigenvalues as a function of gate voltage) for $E_C/E_J = 10$

$$\hat{H} = \hat{K} + \hat{U} \tag{3.15}$$

$$= E_C \left(\hat{n} - n_g\right)^2 - \frac{E_J}{2} \sum_{n \in \mathbb{Z}} \left(|n+1\rangle \langle n| + |n\rangle \langle n+1|\right) \tag{3.16}$$

This hamiltonian can be numerically solved by truncating it to first few charge states. Energy eigenvalues as a function of bias charge n_g is plotted in Figure 3.2 on page 16.

Using the relation $\hat{n} = -i\partial/\partial\theta$, we can write the Cooper pair box hamiltonian in the phase space as follows:

$$\hat{H} = E_C \left(i\frac{\partial}{\partial\theta} + n_g\right)^2 - E_J cos\left(\hat{\theta}\right) \tag{3.17}$$

So that the time-independent Schrödinger equation reads:

$$E_C\left(i\frac{\partial}{\partial\theta}+n_g\right)^2\psi_k(\theta)-E_Jcos(\theta)\,\psi_k(\theta)=E_k\psi(\theta) \tag{3.18}$$

with periodic boundary condition $\psi_k(\theta+2\pi)=\psi(\theta)$. Making the transformation $\varphi_k(\theta)=exp(-in_g\theta)\,\psi_k(\theta)$ [4], Schrödinger equation can be cast in the form:

$$-E_C\frac{\partial^2}{\partial\theta^2}\varphi_k(\theta)-E_Jcos(\theta)\,\varphi_k(\theta)=E_k\varphi_k(\theta) \tag{3.19}$$

which can also be written in the following form:

$$\frac{\partial^2 y(z)}{\partial z^2}-2qcos(2z)\,y(z)=-ay(z) \tag{3.20}$$

with $z=\theta/2$, $y(z)=\varphi_k(2z)$, $q=-2E_J/E_C$, and $a=4E_k/E_C$. This is the well-known Mathieu equation with Mathieu functions as solutions.

Let's now solve Eq. (3.20) numerically and see what happens when we change the ratio q of Josephson energy to the Coulomb energy E_C . The results are plotted in Figure 3.3 on page 18. We observe that ψ_0 becomes more localized as E_J/E_C is increased.

In charge space we see that the inverse of this effect is happening, that is the charge n becomes more localized as the ratio E_J/E_C decreases, see Figure 3.4 on page 18.

The Cooper Pair Box hamiltonian in Eq. (3.16) can be approximated at bias $n_g=0.5$ in the truncated charge basis $\{|0\rangle,|1\rangle\}$ as:

$$\hat{H}=-\frac{1}{2}B_z\hat{\sigma}_z-\frac{1}{2}B_x\hat{\sigma}_x \tag{3.21}$$

where $B_z=E_C(1-2n_g)$ and $B_x=E_J$. B_z can be tuned by the gate voltage. If we replace the single junction with a DC SQUID we can also make B_x tunable. Then by pulsing B_z and B_x one can perform any single qubit operation [9].

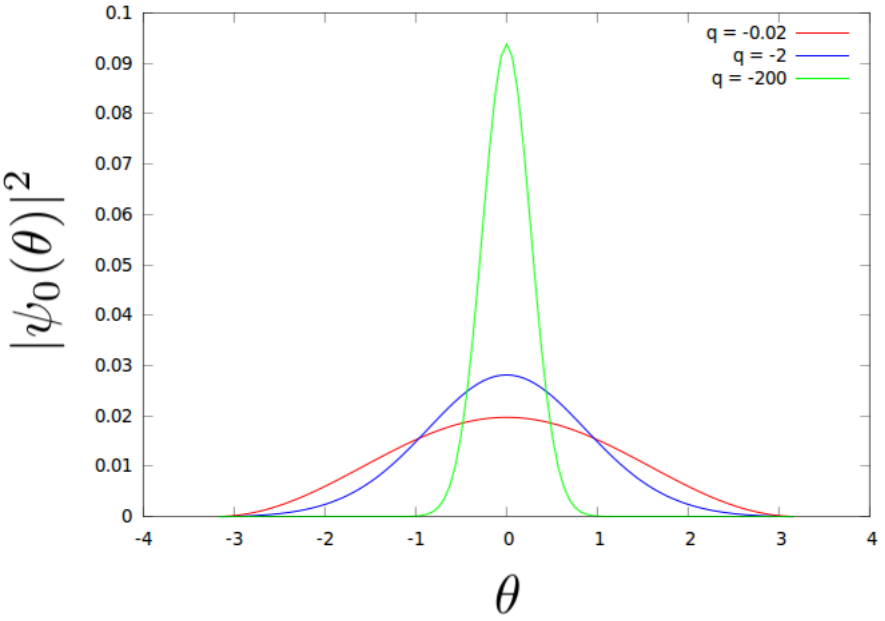

Figure 3.3: Ground state wavefunction as a function of the ratio E_J/E_C

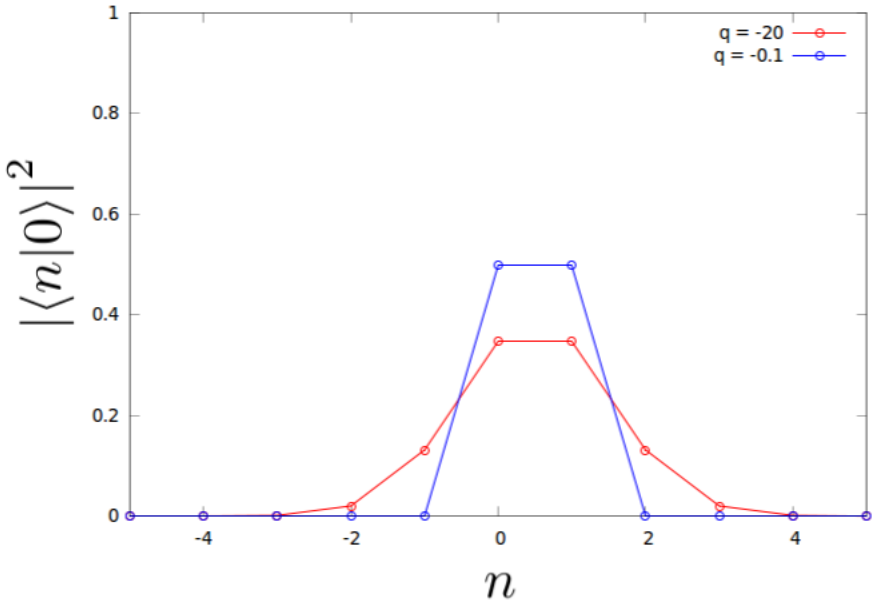

Figure 3.4: Charge distribution as a function of E_J/E_C at $n_g = 0.5$

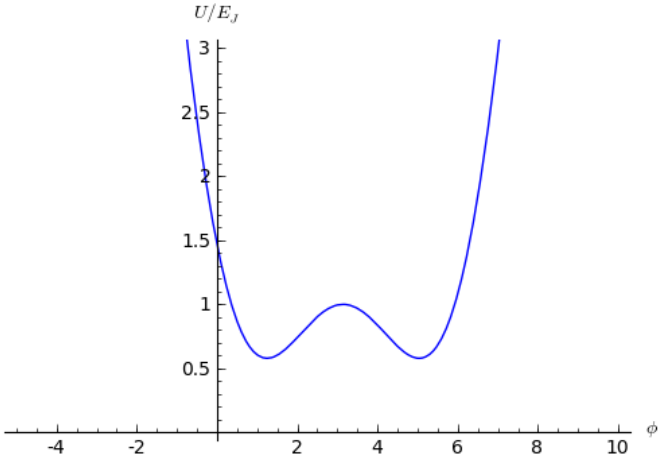

Figure 3.5: RF SQUID double-well potential at $\alpha = 0.5$ and $\phi_x = \pi$

3.2 Flux Qubits

3.2.1 RF SQUID

RF SQUID is the simplest flux qubit formed by a josephson junction in a superconducting loop of self inductance L as shown in Figure 1.1 on page 3. It has been studied in various contexts such as macroscopic verification of quantum tunneling [1]. An external flux Φ_x is applied to bias the circuit. Applying circuit quantization rules discussed in Section 2.1, one gets the following hamiltonian for RF SQUID circuit:

$$\hat{H} = -E_J cos\left(2\pi\hat{\Phi}/\Phi_0\right) + \frac{\left(\hat{\Phi} - \Phi_x\right)^2}{2L} + \frac{\hat{Q}^2}{2C_J} \tag{3.22}$$

where $\hat{\Phi}$ is the flux across the junction and $\hat{Q}$ the charge on junction's capacitance C_J. They satisfy $\left[\hat{\Phi}, \hat{Q}\right] = ih$. If self-inductance L of the loop is large enough such that $E_J > \frac{\Phi_0^2}{4\pi^2 L}$, around the bias point $\Phi_x = \Phi_0/2$ the potential energy $\hat{U} = -E_J cos\left(2\pi\hat{\Phi}/\Phi_0\right) + \frac{\left(\hat{\Phi}-\Phi_x\right)^2}{2L}$ forms a double well as shown in Figure 3.5 on page 19.

One can rewrite the potential in Eq. (3.22) as:

$$\hat{U} = E_J \left[-cos\left(\hat{\phi}\right) + \alpha \frac{\left(\hat{\phi} - \phi_x\right)^2}{2} \right] \tag{3.23}$$

where $\hat{\phi} = 2\pi \frac{\hat{\Phi}}{\Phi_0}$, $\phi_x = 2\pi \frac{\Phi_x}{\Phi_0}$ and $\alpha = \frac{\Phi_0^2}{4\pi^2 L E_J}$.

The bias point ϕ_x determines the asymmetry of the wells. At the degeneracy point $\phi_x = \pi$, the double well potential is symmetric. The two minima at $\phi = \phi_L$ and $\phi = \phi_R$ correspond to persistent currents flowing in the loop. If we move ϕ_x slightly away from the degeneracy point $\phi_x = \pi$ we can make one well higher than the other.

To find the energy eigenstates of the system, one can solve the time-independent Schrödinger equation numerically. The results is shown in Figure 3.6 on page 21. The ground state and the first excited state are symmetric and anti-symmetric combinations of localized ground states of each well, respectively.

Another way to solve for eigenstates is to make a "tight-binding" approximation. Assume that ground states $|L\rangle$ and $|R\rangle$ corresponding to each well do not overlap. One can make a two-level approximation by choosing those two states as basis to write the hamiltonian:

$$\hat{H} = \begin{bmatrix} E_L & -t \\ -t & E_R \end{bmatrix} \tag{3.24}$$

where $E_L = \langle L| \hat{H} |L\rangle$, $E_R = \langle R| \hat{H} |R\rangle$ and $\langle L| \hat{H} |R\rangle = -t$ the tunneling amplitude between wells. Taking $(E_L + E_R)/2$ as the zero of energy the hamiltonian becomes:

$$\hat{H} = \begin{bmatrix} \Delta E/2 & -t \\ -t & -\Delta E/2 \end{bmatrix} \tag{3.25}$$

where $\Delta E = E_L - E_R$. We can now diagonalize this hamiltonian to find the eigenvalues and eigenstates. To do this construct the rotation matrix [5]:

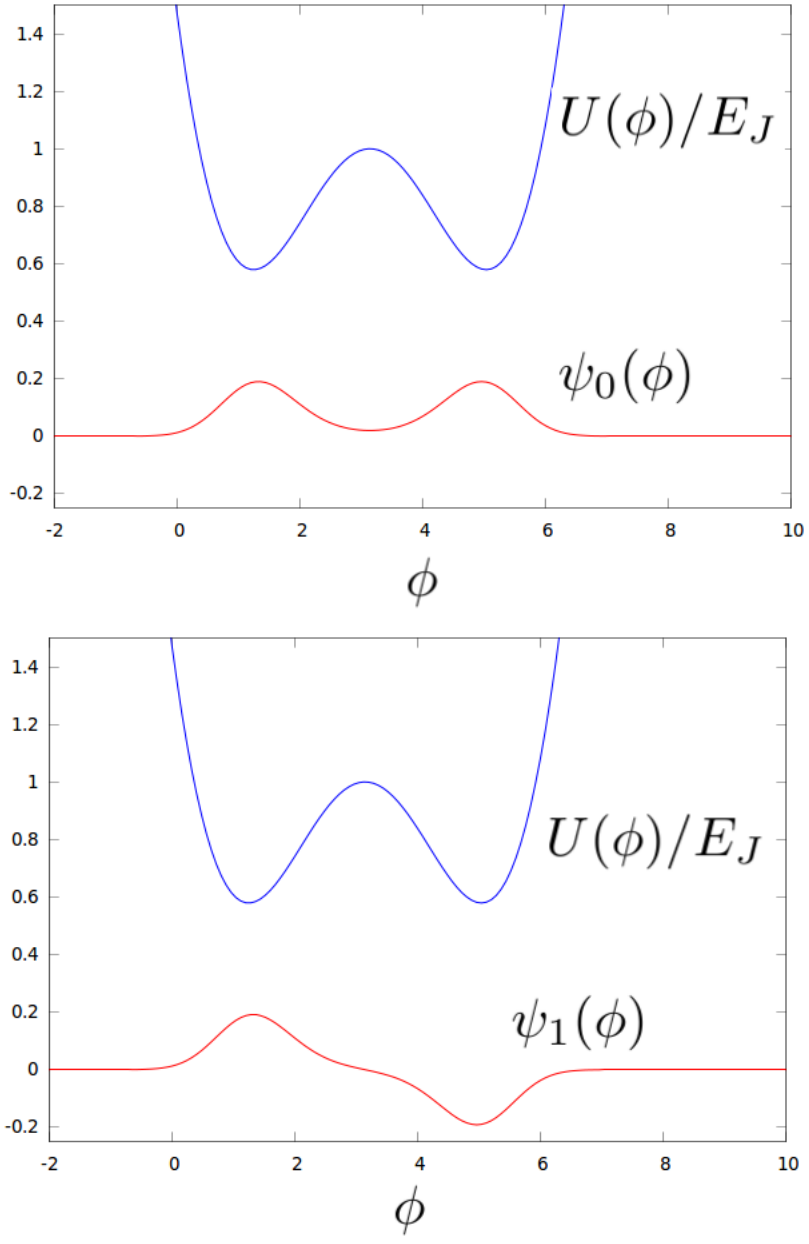

Figure 3.6: Ground-state and first excited state wavefunctions of RF SQUID for $\alpha = 0.5$ and $\phi_x = \pi$

$$D = \begin{bmatrix} cos\,(\theta/2) & -sin\,(\theta/2) \\ sin\,(\theta/2) & cos\,(\theta/2) \end{bmatrix} \tag{3.26}$$

where $\theta = -arctan(2t/\Delta E)$. In the eigenstate basis the hamiltonian becomes:

$$\hat{H}' = D^T \hat{H} D = -\sqrt{(\Delta E/2)^2 + t^2}\sigma_z \tag{3.27}$$

with eigenvalues $E_0 = -\sqrt{(\Delta E/2)^2 + t^2}$ and $E_1 = +\sqrt{(\Delta E/2)^2 + t^2}$. The eigenstates $|0\rangle$, $|1\rangle$ corresponds to the columns of D :

$$|0\rangle = \frac{1}{\sqrt{2}}\left(\sqrt{1 - \frac{\Delta E/2}{\sqrt{(\Delta E/2)^2 + t^2}}}\,|L\rangle + \sqrt{1 + \frac{\Delta E/2}{\sqrt{(\Delta E/2)^2 + t^2}}}\,|R\rangle\right) \tag{3.28}$$

$$|1\rangle = \frac{1}{\sqrt{2}}\left(\sqrt{1 + \frac{\Delta E/2}{\sqrt{(\Delta E/2)^2 + t^2}}}\,|L\rangle - \sqrt{1 - \frac{\Delta E/2}{\sqrt{(\Delta E/2)^2 + t^2}}}\,|R\rangle\right) \tag{3.29}$$

We see that the eigenstates are superpositions of the single-well ground states due to tunneling. At the degeneracy point $\phi_x = \pi$, the potential is symmetric so that $\Delta E = 0$ and $\theta = -\pi/2$. In this case, eigenvalues are $E_0 = -t$, $E_1 = t$ and the eigenvectors are $|0\rangle = \frac{1}{\sqrt{2}}(|L\rangle + |R\rangle)$, $|1\rangle = \frac{1}{\sqrt{2}}(|L\rangle - |R\rangle)$.

One can tune the height of the barrier between the wells by changing α. This in turn will change tunneling amplitude t. We can tune α by changing the Josephson energy E_J. To change E_J replace the single Josephson junction with a DC SQUID consisting of two josephson junctions in a superconducting loop threaded by an external flux Φ_x'. DC SQUID will behave effectively as a single junction with josephson energy $E_J' = 2E_J cos\,(\pi\Phi_x'/\Phi_0)$ (see the Appendix).

Now assume that we have slightly biased the circuit from the degeneracy point to a new operating point defined by the angle $\theta = -arctan(2t/\Delta E)$ and the eigen-

energies $\pm\sqrt{(\Delta E/2)^2 + t^2}$. Note that in this case $|\Delta E/2| \gg t$ so that $\theta \approx 0$ and the eigenstates collapse to the localized states in each well. Any further change in external fluxes Φ_x and Φ'_x will change matrix elements of the hamiltonian by δ and Δt respectively:

$$\hat{H} = \begin{bmatrix} \Delta E/2 + \delta & -t + \Delta t \\ -t + \Delta t & -\Delta E/2 - \delta \end{bmatrix} \tag{3.30}$$

or in the eigenstate basis:

$$\hat{H}' = -\sqrt{(\Delta E/2)^2 + t^2}\sigma_z + \Delta H \tag{3.31}$$

where $\Delta H = \delta\,(cos\theta\sigma_z - sin\theta\sigma_x) - \Delta t\,(sin\theta\sigma_z + cos\theta\sigma_x)$. This way one can change the state of the qubit and perform any single qubit operation [9].

3.2.2 Delft qubit

Now let's increase the complexity a bit. Delft qubit has three Josephson junctions interrupting a superconducting loop as shown in Figure 3.7 on page 24. The junctions 1 and 2 are identical: $E_{J1} = E_{J2} = E_J$ and $C_1 = C_2 = C$, whereas the third junction in the middle has energy $E_{J3} = \alpha E_J$ and capacitance $C_3 = \alpha C$. Again an external magnetic field $\Phi_x = f\Phi_0$ is applied to bias the circuit. The loop is assumed to have negligible self inductance. Delft qubit requires a much smaller loop then RF SQUID hence less coupling to the flux noise [9].

To write the hamiltonian of the circuit, we follow the procedure described in Section 2.1 and introduce node fluxes $\hat{\Phi}_1$, $\hat{\Phi}_2$ and node charges $\hat{Q}_1$, $\hat{Q}_2$. Those variables are independent variables corresponding to our choice of the spanning tree and they satisfy commutation relations $\left[\hat{\Phi}_1, \hat{Q}_1\right] = i\hbar$, $\left[\hat{\Phi}_2, \hat{Q}_2\right] = i\hbar$. To find the kinetic

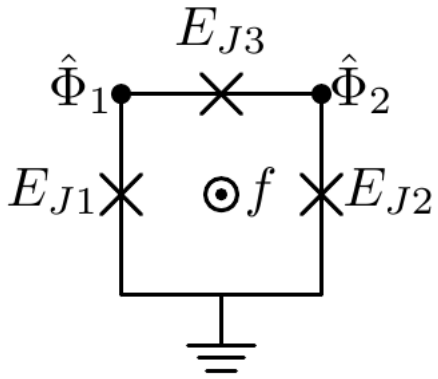

Figure 3.7: The Delft qubit

energy term, we need the capacitance matrix [6]. The reduced capacitance matrix reads:

$$C = \begin{bmatrix} C_1 + C_3 & -C_3 \\ -C_3 & C_2 + C_3 \end{bmatrix} = C \begin{bmatrix} 1+\alpha & -\alpha \\ -\alpha & 1+\alpha \end{bmatrix} \tag{3.32}$$

Electrostatic energy stored in the circuit is then:

$$\hat{K} = \frac{1}{2}\hat{Q}^T C^{-1} \hat{Q} \tag{3.33}$$

$$= \frac{1}{2C(1+2\alpha)} \left((1+\alpha)\,\hat{Q}_1^2 + 2\alpha \hat{Q}_1 \hat{Q}_2 + (1+\alpha)\,\hat{Q}_2^2 \right) \tag{3.34}$$

Potential energy of the system is the sum of the josephson energies:

$$\hat{U} = -E_J cos\left(2\pi\hat{\Phi}_1/\Phi_0\right) - E_J cos\left(2\pi\hat{\Phi}_2/\Phi_0\right) - \alpha E_J cos\left(2\pi\hat{\Phi}_3/\Phi_0\right) \tag{3.35}$$

We have also the following constraint for the fluxes around the loop:

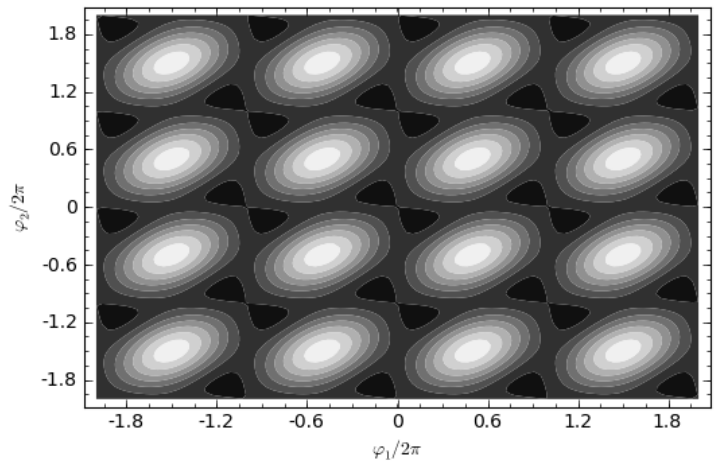

Figure 3.8: Contour plot of the potential energy for $\alpha = 0.8$ and $f = 1/2$

$$\hat{\Phi}_1 - \hat{\Phi}_2 + \hat{\Phi}_3 + \Phi_x = 0 \tag{3.36}$$

With this constraint for fluxes around the loop we can rewrite the potential energy as:

$$\hat{U} = E_J \left[-cos\left(\hat{\varphi}_1\right) - cos\left(\hat{\varphi}_2\right) - \alpha cos\left(2\pi f + \hat{\varphi}_1 - \hat{\varphi}_2\right) \right] \tag{3.37}$$

where we have defined $\hat{\varphi}_i = \frac{2\pi}{\Phi_0}\hat{\Phi}_i$ for $i = 1, 2, 3$. For $\alpha > 1/2$, near $f = 1/2$ this potential has two stable minima with same energy corresponding to currents circulating in the loop in opposite directions [5]. The contour plot of the potential is given in Figure 3.8 on page 25 for $\alpha = 0.8$ where we see the two minima at $\varphi_1 = -\varphi_2 = \varphi^*$ with $cos\left(\varphi^*\right) = 1/2\alpha$ repeated in a square lattice [5]. The barrier between minima within the same unit cell is higher than the barrier between minima between nearest neighbor cells which will suppress tunneling between cells.

To diagonalize the capacitance matrix we make a canonical change of coordinates:

$$\hat{\Phi}_+ = \left(\hat{\Phi}_1 + \hat{\Phi}_2\right)/2 \tag{3.38}$$

$$\hat{\Phi}_- = \left(\hat{\Phi}_1 - \hat{\Phi}_2\right)/2 \tag{3.39}$$

Momenta change accordingly to preserve commutation relations:

$$\hat{Q}_+ = \hat{Q}_1 + \hat{Q}_2 \tag{3.40}$$

$$\hat{Q}_- = \hat{Q}_1 - \hat{Q}_2 \tag{3.41}$$

The hamiltonian in the new coordinates reads:

$$\hat{H} = \frac{\hat{Q}_+^2}{4C} + \frac{\hat{Q}_-^2}{4C(1+2\alpha)} \tag{3.42}$$

$$+ E_J\left[-2cos\left(2\pi\hat{\Phi}_+/\Phi_0\right)cos\left(2\pi\hat{\Phi}_-/\Phi_0\right)\right] \tag{3.43}$$

$$- E_J\alpha cos\left(2\pi\Phi_x/\Phi_0 + 2\hat{\Phi}_-\right) \tag{3.44}$$

Or in terms of the phases $\hat{\varphi}_\pm = 2\pi\hat{\Phi}_\pm/\Phi_0$ such that $\hat{Q}_\pm = -i\hbar\left(\frac{2\pi}{\Phi_0}\right)\frac{\partial}{\partial\varphi_\pm}$ at $f = 0.5$:

$$\hat{H} = \frac{\hat{Q}_+^2}{4C} + \frac{\hat{Q}_-^2}{4C(1+2\alpha)}$$

$$+ E_J\left[\alpha cos\left(2\hat{\varphi}_-\right) - 2cos\left(\hat{\varphi}_+\right)cos\left(\hat{\varphi}_-\right)\right] \tag{3.45}$$

Now let's numerically solve this hamiltonian over a grid in phase variable space and plot the wavefunctions corresponding to the first two energy eigenvalues. The results are presented in Figure 3.9 on page 27.

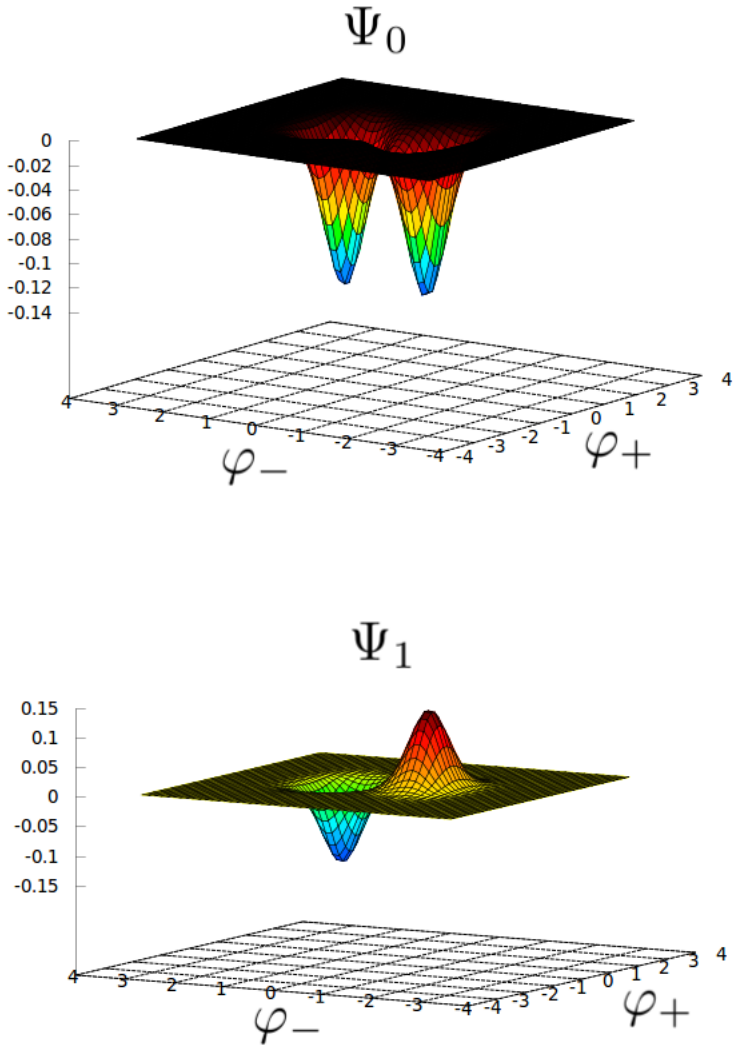

Figure 3.9: First two eigenstates Ψ_0 and Ψ_1 of the Delft qubit

As in the case of the RF SQUID we can again make a tight-binding approximation and choose the localized states in each well as our basis and write the hamiltonian in this basis as in Eq. (3.24). Note that all the discussion about the manipulation of the RF SQUID applies here. By tuning external bias f or the parameter α by using a DC SQUID instead of the third junction, we can still arrive at the hamiltonian in Eq. (3.31) which means that we can perform any single qubit operation with the Delft qubit. Typical value of energy splitting between the two states is about 10 GHz at bias $f = 0.495$ [5].

Chapter 4

COUPLING QUBITS TO TRANSMISSION LINES

In this section we will explore some coupling schemes proposed in [7] between the Delft qubit and a transmission line. The coupling will be tunable such that we will be able to turn it on and off via external fluxes. We will also be able to change the type of coupling so that the flux across the transmission line will couple to the x or z components of the spin.

We start with the most basic coupling scheme where the qubit is directly coupled to the line as shown in Figure 4.1 on page 29. Here $\Delta\hat{\psi}$ is related to the flux $\Delta\hat{\Phi}$ across the transmission line by $\Delta\hat{\psi} = \frac{2\pi}{\Phi_0}\Delta\hat{\Phi}$. Potential part of the qubit hamiltonian reads:

$$\hat{U} = E_J\left[-cos\left(\hat{\varphi}_1\right) - cos\left(\hat{\varphi}_2\right) - \alpha cos\left(\hat{\varphi}_3\right)\right] \tag{4.1}$$

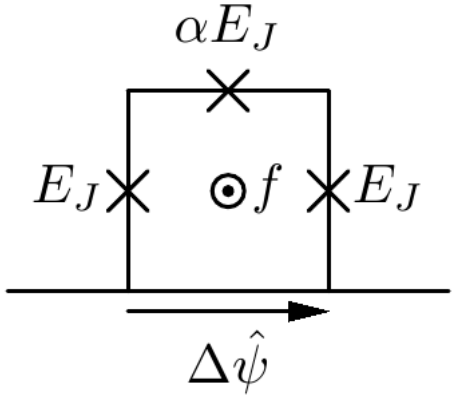

Figure 4.1: Basic coupling to the transmission line

Equating fluxes around the loop we get:

$$\hat{\varphi}_1 - \hat{\varphi}_2 + \hat{\varphi}_3 - \Delta\hat{\psi} = f \tag{4.2}$$

Using Eq. (4.2) with flux bias $f = \pi$ qubit potential becomes:

$$\hat{U} = E_J \left[-cos\left(\hat{\varphi}_1\right) - cos\left(\hat{\varphi}_2\right) - \alpha cos\left(\pi + \Delta\hat{\psi} - \left(\hat{\varphi}_1 - \hat{\varphi}_2\right)\right)\right] \tag{4.3}$$

In sum and difference coordinates $\hat{\varphi}_\pm = \left(\hat{\varphi}_1 \pm \hat{\varphi}_2\right)/2$ the potential reads:

$$\begin{aligned} \hat{U} &= E_J \left[\alpha cos\left(2\hat{\varphi}_- - \Delta\hat{\psi}\right) - 2cos\left(\hat{\varphi}_+\right) cos\left(\hat{\varphi}_-\right)\right] && (4.4)\\ &= E_J \left[\alpha cos\left(2\hat{\varphi}_-\right) - 2cos\left(\hat{\varphi}_+\right) cos\left(\hat{\varphi}_-\right)\right] && (4.5)\\ &+ \alpha E_J sin\left(2\hat{\varphi}_-\right)\Delta\hat{\psi} && (4.6) \end{aligned}$$

to the first order in $\Delta\hat{\psi}$. We identify Eq. (4.5) with the qubit hamiltonian in Eq. (3.45) and Eq. (4.6) is the first order coupling term. Note that the line flux $\Delta\hat{\psi}$ couples directly to the current $\hat{I} = \frac{2\pi}{\Phi_0}\alpha E_J sin\left(2\hat{\varphi}_-\right)$ circulating in the loop. We compute matrix elements of the operator $sin\left(2\hat{\varphi}_-\right)$ in the qubit basis as usual:

$$\begin{aligned} \langle 0| sin\left(2\hat{\varphi}_-\right)|0\rangle &= \int\int d\varphi_+ d\varphi_- \left|\Psi_0\left(\varphi_+,\varphi_-\right)\right|^2 sin\left(2\varphi_-\right) = 0 && (4.7)\\ \langle 1| sin\left(2\hat{\varphi}_-\right)|1\rangle &= \int\int d\varphi_+ d\varphi_- \left|\Psi_1\left(\varphi_+,\varphi_-\right)\right|^2 sin\left(2\varphi_-\right) = 0 && (4.8)\\ \langle 0| sin\left(2\hat{\varphi}_-\right)|1\rangle &= \int\int d\varphi_+ d\varphi_- \Psi_0^*\left(\varphi_+,\varphi_-\right)\Psi_1\left(\varphi_+,\varphi_-\right) sin\left(2\varphi_-\right) && (4.9)\\ &\simeq \sqrt{1 - \frac{1}{4\alpha^2}} && (4.10) \end{aligned}$$

Equations (4.7) and (4.8) follow from the fact that $sin\left(2\varphi_-\right)$ is an odd function of

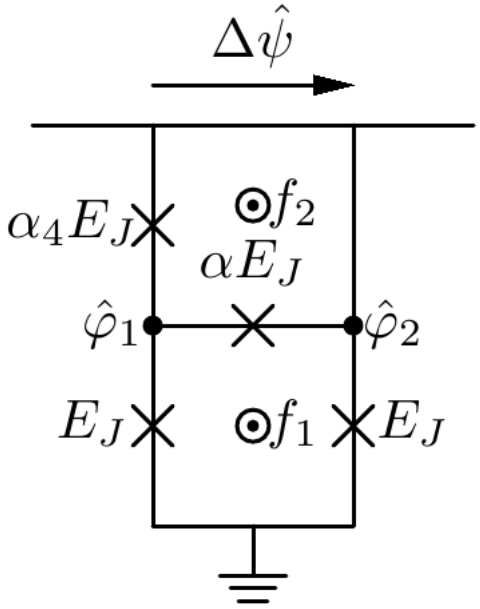

Figure 4.2: Improved coupling scheme

φ_- whereas $|\Psi_0(\varphi_+,\varphi_-)|^2$ and $|\Psi_1(\varphi_+,\varphi_-)|^2$ are even functions of φ_-. Equation (4.10) follows from the fact that at potential minima $cos\left(2\varphi_-^*\right) = 1/2\alpha$ and from the assumption of localized single well wavefunctions. Now the hamiltonian including the qubit and coupling terms reads in the qubit basis:

$$\hat{H} = E_q\hat{\sigma}_z + \alpha\sqrt{1-\frac{1}{4\alpha^2}}E_J\hat{\sigma}_x\Delta\hat{\psi} \tag{4.11}$$

where E_q is the qubit frequency which depends on the tunneling between potential minima. Note that in this scheme coupling strength depends on the qubit parameter α . Also the coupling is fixed at $\hat{\sigma}_x\Delta\hat{\psi}$ and there is no way to tune the coupling type.

The above coupling scheme can be improved by adding a loop with a fourth junction between the qubit and the transmission line as shown in Figure 4.2 on page 31.

In this setting the qubit potential reads:

$$\hat{U} = E_J \left[-cos\left(\hat{\varphi}_1\right) - cos\left(\hat{\varphi}_2\right) - \alpha cos\left(\hat{\varphi}_3\right) - \alpha_4 cos\left(\hat{\varphi}_4\right) \right] \tag{4.12}$$

Kirchhoff's voltage law around the loops gives:

$$\hat{\varphi}_1 - \hat{\varphi}_2 + \hat{\varphi}_3 + f_1 = 0 \tag{4.13}$$

$$-\hat{\varphi}_3 + \hat{\varphi}_4 - \Delta\hat{\psi} + f_2 = 0 \tag{4.14}$$

With above constraints we rewrite the qubit potential as a function of sum and difference coordinates:

$$\begin{aligned}
\hat{U} &= E_J \left[-cos\left(\hat{\varphi}_1\right) - cos\left(\hat{\varphi}_2\right) - \alpha cos\left(\hat{\varphi}_3\right) - \alpha_4 cos\left(\hat{\varphi}_4\right) \right] && (4.15)\\
&= E_J \left[-cos\left(\hat{\varphi}_1\right) - cos\left(\hat{\varphi}_2\right) - \alpha cos\left(\hat{\varphi}_1 - \hat{\varphi}_2 + f_1\right) \right] && (4.16)\\
&- \alpha_4 E_J cos\left(\hat{\varphi}_1 - \hat{\varphi}_2 - \Delta\hat{\psi} + f_1 + f_2\right) && (4.17)\\
&= E_J \left[-\alpha cos\left(2\hat{\varphi}_- + f_1\right) - 2cos\left(\hat{\varphi}_+\right) cos\left(\hat{\varphi}_-\right) \right] && (4.18)\\
&- \alpha_4 E_J cos\left(2\hat{\varphi}_- - \Delta\hat{\psi} + f_1 + f_2\right) && (4.19)
\end{aligned}$$

At bias point $f_1 = f_2 = \pi$, to the first order in $\Delta\hat{\psi}$:

$$\begin{aligned}
\hat{U} &= E_J \left[\alpha cos\left(2\hat{\varphi}_-\right) - 2cos\left(\hat{\varphi}_+\right) cos\left(\hat{\varphi}_-\right) \right] && (4.20)\\
&- \alpha_4 E_J cos\left(2\hat{\varphi}_- - \Delta\hat{\psi}\right) && (4.21)\\
&= E_J \left[\left(\alpha - \alpha_4\right) cos\left(2\hat{\varphi}_-\right) - 2cos\left(\hat{\varphi}_+\right) cos\left(\hat{\varphi}_-\right) \right] && (4.22)\\
&- \alpha_4 E_J sin\left(2\hat{\varphi}_-\right) \Delta\hat{\psi} && (4.23)
\end{aligned}$$

Defining $\alpha' = \alpha - \alpha_4$ we see that qubit potential is independent of the coupling term: coupling strength can be tuned by changing α_4 whereas qubit parameter α' can be adjusted independently by changing α . The hamiltonian in the qubit basis reads:

$$\hat{H} = E_q \hat{\sigma}_z + \alpha_4 \sqrt{1 - \frac{1}{4\alpha'^2}} E_J \hat{\sigma}_x \Delta\hat{\psi} \tag{4.24}$$

Consider now the case where f_2 is fixed at $f_2 = \pi$ and we move f_1 away from π slightly such that $f_1 = \pi + \Delta f$. In this case the potential reads:

$$\begin{aligned}
\hat{U} &= E_J \left[\alpha cos\left(2\hat{\varphi}_- + \Delta f\right) - 2cos\left(\hat{\varphi}_+\right) cos\left(\hat{\varphi}_-\right)\right] && (4.25)\\
&- \alpha_4 cos\left(2\hat{\varphi}_- + \Delta f - \Delta\hat{\psi}\right) && (4.26)\\
&= E_J \left[\alpha' cos\left(2\hat{\varphi}_- + \Delta f\right) - 2cos\left(\hat{\varphi}_+\right) cos\left(\hat{\varphi}_-\right)\right] && (4.27)\\
&- \alpha_4 E_J sin\left(2\hat{\varphi}_- + \Delta f\right) \Delta\hat{\psi} && (4.28)\\
&= E_J \left[\alpha' cos\left(2\hat{\varphi}_- + \Delta f\right) - 2cos\left(\hat{\varphi}_+\right) cos\left(\hat{\varphi}_-\right)\right] && (4.29)\\
&- \alpha_4 E_J \left[cos\left(\Delta f\right) sin\left(2\hat{\varphi}_-\right) + sin\left(\Delta f\right) cos\left(2\hat{\varphi}_-\right)\right] \Delta\hat{\psi} && (4.30)
\end{aligned}$$

Note that the flux Δf will rotate the qubit so that the new eigenstates will be the localized states in each well. Assuming $\Delta f \ll 1$, the potential is:

$$\begin{aligned}
\hat{U} &\approx E_J \left[\alpha' cos\left(2\hat{\varphi}_- + \Delta f\right) - 2cos\left(\hat{\varphi}_+\right) cos\left(\hat{\varphi}_-\right)\right] && (4.31)\\
&- \alpha_4 E_J sin\left(2\hat{\varphi}_-\right) \Delta\hat{\psi} && (4.32)
\end{aligned}$$

In this new basis the matrix elements of the operator $sin\left(2\hat{\varphi}_-\right)$ are:

$$\langle 0| sin\left(2\hat{\varphi}_-\right)|0\rangle = \int\int d\varphi_+ d\varphi_- \left|\Psi_0\left(\varphi_+,\varphi_-\right)\right|^2 sin\left(2\varphi_-\right) \tag{4.33}$$

$$\simeq -\sqrt{1-\frac{1}{4\alpha'^2}} \tag{4.34}$$

$$\langle 1| sin\left(2\hat{\varphi}_-\right)|1\rangle = \int\int d\varphi_+ d\varphi_- \left|\Psi_1\left(\varphi_+,\varphi_-\right)\right|^2 sin\left(2\varphi_-\right) \tag{4.35}$$

$$\simeq \sqrt{1-\frac{1}{4\alpha'^2}} \tag{4.36}$$

$$\langle 0| sin\left(2\hat{\varphi}_-\right)|1\rangle = \int\int d\varphi_+ d\varphi_- \Psi_0^*\left(\varphi_+,\varphi_-\right)\Psi_1\left(\varphi_+,\varphi_-\right) sin\left(2\varphi_-\right) \tag{4.37}$$

$$= 0 \tag{4.38}$$

So the hamiltonian in the new qubit basis reads:

$$\hat{H} = E_q\hat{\sigma}_z + \alpha_4\sqrt{1-\frac{1}{4\alpha'^2}}E_J\hat{\sigma}_z\Delta\hat{\psi} \tag{4.39}$$

Note that the interaction rotated from $\hat{\sigma}_x$ to $\hat{\sigma}_z$.

Now let's increase the complexity of the circuit a bit further and look at the following design in Figure 4.3 on page 35:

Here we have added a third loop and a fifth junction with $\alpha_5 = \alpha_4$. We will work at bias fluxes $f_3 = \pi - f_1 - f_2$. Fluxes around the third loop are constrained by:

$$-\hat{\varphi}_1 + \hat{\varphi}_2 + \hat{\varphi}_5 + f_3 = 0 \tag{4.40}$$

Now the potential due to junctions reads:

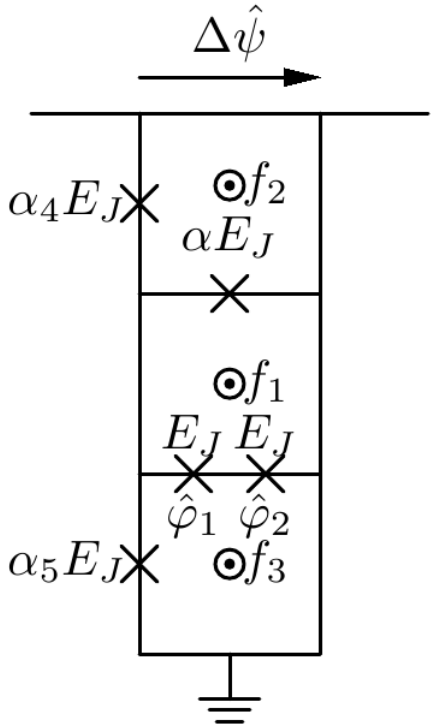

Figure 4.3: Coupling circuit with three loops

$$\hat{U} = E_J\left[-cos\left(\hat{\varphi}_1\right) - cos\left(\hat{\varphi}_2\right) - \alpha cos\left(\hat{\varphi}_3\right)\right] \tag{4.41}$$

$$- \alpha_4 E_J cos\left(\hat{\varphi}_4\right) - \alpha_4 E_J cos\left(\hat{\varphi}_5\right) \tag{4.42}$$

$$= E_J\left[-cos\left(\hat{\varphi}_1\right) - cos\left(\hat{\varphi}_2\right) - \alpha cos\left(\hat{\varphi}_1 - \hat{\varphi}_2 + f_1\right)\right] \tag{4.43}$$

$$- \alpha_4 E_J cos\left(\hat{\varphi}_1 - \hat{\varphi}_2 - \Delta\hat{\psi} + f_1 + f_2\right) \tag{4.44}$$

$$+ \alpha_4 E_J cos\left(-\hat{\varphi}_1 + \hat{\varphi}_2 - f_1 - f_2\right) \tag{4.45}$$

$$= E_J\left[-\alpha cos\left(2\hat{\varphi}_- + f_1\right) - 2cos\left(\hat{\varphi}_+\right) cos\left(\hat{\varphi}_-\right)\right] \tag{4.46}$$

$$- \alpha_4 E_J cos\left(2\hat{\varphi}_- - \Delta\hat{\psi} + f_1 + f_2\right) + \alpha_4 E_J cos\left(2\hat{\varphi}_- + f_1 + f_2\right) \tag{4.47}$$

Note that in this model we have the freedom to change f_2 as we wish. Again assuming $f_1 = \pi + \Delta f$, to the first order in $\Delta\hat{\psi}$ we have :

$$\hat{U} = E_J \left[\alpha cos\left(2\hat{\varphi}_- + \Delta f\right) - 2cos\left(\hat{\varphi}_+\right) cos\left(\hat{\varphi}_-\right)\right] \tag{4.48}$$

$$+ \quad \alpha_4 E_J sin\left(2\hat{\varphi}_- + \Delta f + f_2\right) \Delta\hat{\psi} \tag{4.49}$$

Let's assume for the moment that $\Delta f = 0$. In this case:

$$\hat{U} = E_J \left[\alpha cos\left(2\hat{\varphi}_-\right) - 2cos\left(\hat{\varphi}_+\right) cos\left(\hat{\varphi}_-\right)\right] \tag{4.50}$$

$$+ \quad \alpha_4 E_J \left[cos\left(f_2\right) sin\left(2\hat{\varphi}_-\right) + sin\left(f_2\right) cos\left(2\hat{\varphi}_-\right)\right] \Delta\hat{\psi} \tag{4.51}$$

Note that the qubit potential in Eq. (4.50) is independent of f_2 and the qubit is in the original basis of symmetric and anti-symmetric wavefunctions. In this basis effective part of the coupling term of Eq. (4.51) is (with a vanishing coupling at $f_2 = \pi/2$!):

$$\hat{H}_c = \alpha_4 E_J cos\left(f_2\right) sin\left(2\hat{\varphi}_-\right) \Delta\hat{\psi} = \alpha_4 \sqrt{1 - \frac{1}{4\alpha^2}} E_J cos\left(f_2\right) \hat{\sigma}_x \Delta\hat{\psi} \tag{4.52}$$

Typical values for the coupling strength are in the range of 500 MHz - 10 GHz for a typical junction of josephson energy 250 GHz [7].

Chapter 5

PROTECTING QUBITS WITH FREQUENCY MODULATION

5.1 Introduction

Frequency Modulation (FM) is one of the analog modulation methods used by electrical engineers to transmit message signals over radio links. It works by changing the frequency of a carrier signal in proportion to the message signal around a carrier frequency ω_c (see Figure 5.1 on page 38). FM has a good noise performance which suppress noise exponentially for a linear increase in bandwidth. One can exploit this feature of FM for the design of qubits more resistant to noise.

By the fluctuation-dissipation theorem [13], noise is the result of random force fluctuations acting on the system and dissipating its coherent energy. So one should find ways to shield the qubit from the noise produced by the macroscopic environment for longer decoherence times.

In superconducting circuits an example of noisy environment is a DC SQUID used for the measurement of the qubit state by inductive coupling. In a continuous type of measurement one should require the decoherence time of the qubit to be larger than the measurement time [14]. Such a system is similar to a communication channel where information flows from qubit to SQUID and the noise flows in the opposite direction. In this paper we propose to FM modulate the qubit degree of freedom before connecting it to the measurement device as shown in Figure 5.2 on page 39. This way the macroscopic device will only interact with the FM modulated signal and

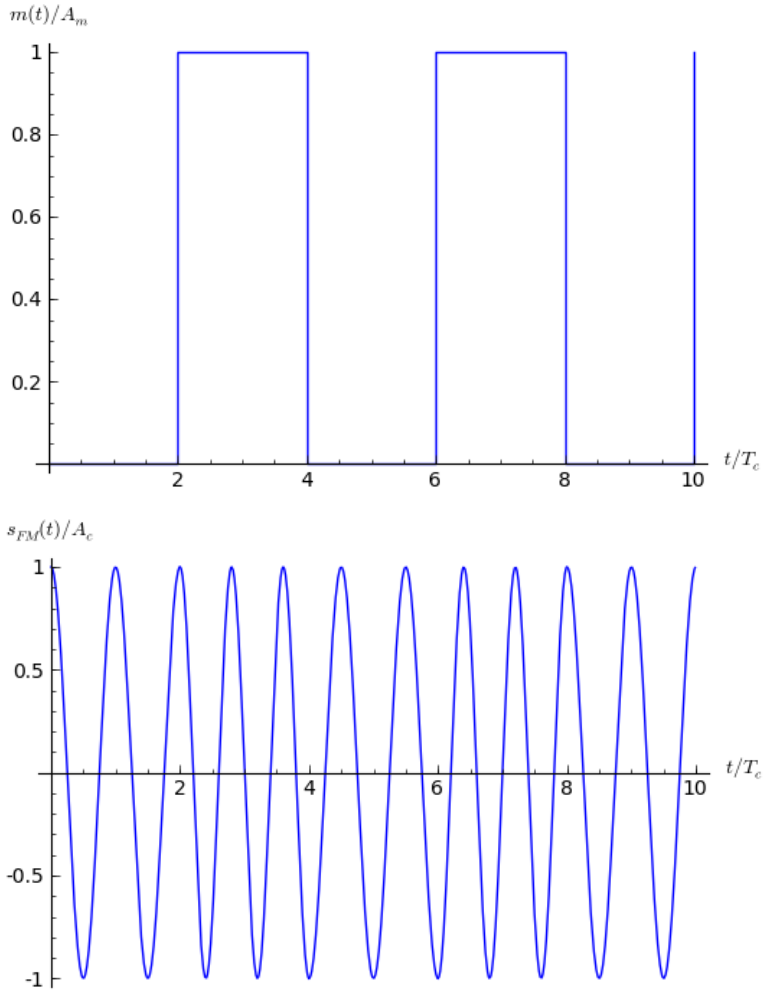

Figure 5.1: FM with $\omega_c = 2\omega_m$ and $c_f = \frac{\omega_c}{4A_m}$ so that $\Delta\omega = 0.25\omega_c$

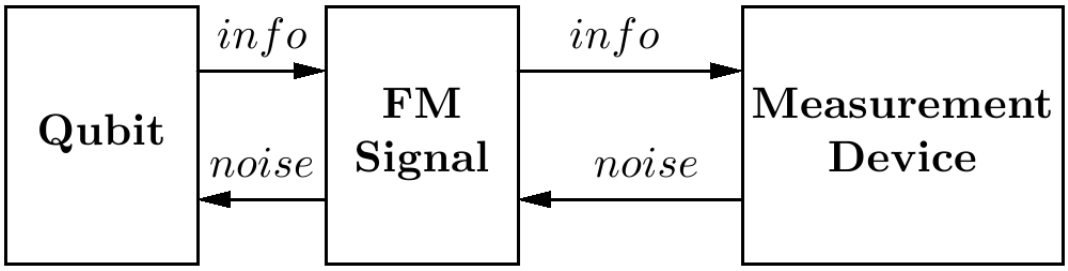

Figure 5.2: FM system for qubits

the noise propagation to the qubit part will be suppressed.

In the following we first review the traditional FM and then propose a model to implement the FM modulation as a dynamical system composed of two oscillators coupled in a nonlinear way.

5.2 Classical Frequency Modulation (FM)

We can write an FM modulated signal in mathematical terms as follows:

$$s_{FM}(t) = A_c cos\left(\omega_c t + c_f \int m(t)\, dt\right) \tag{5.1}$$

Here A_c is the amplitude of the carrier signal, c_f is a parameter which determines the frequency deviation around the carrier frequency ω_c and $m(t)$ is the message signal. The instantaneous frequency ω_i of the FM signal $s_{FM}(t)$ is obtained simply by taking the derivative of the argument of the cosine function which gives:

$$\omega_i = \omega_c + c_f m(t) \tag{5.2}$$

which is proportional to $m(t)$ around ω_c.

For a sinusoidal message signal $m(t) = A_m cos(\omega_m t)$ at some frequency ω_m , we

have:

$$\omega_i = \omega_c + \Delta\omega cos\left(\omega_m t\right) \tag{5.3}$$

where $\Delta\omega = c_f A_m$ is the frequency deviation. The frequency ω_m of the message signal determines the rate at which the frequency deviates from ω_c. In the following we will assume that $\Delta\omega \ll \omega_c$.

An important parameter for FM modulation is the modulation index β defined by:

$$\beta = \frac{\Delta\omega}{\omega_m} \tag{5.4}$$

For a single tone message signal $m\left(t\right) = A_m cos\left(\omega_m t\right)$ the bandwidth BW of the FM signal in Eq. 5.1 can be estimated by Carson's Rule:

$$BW \simeq 2\omega_m\left(1+\beta\right)$$

For a more general message signal $m\left(t\right)$ one can redefine the modulation index β:

$$\beta = \frac{\Delta\omega}{\omega_{max}} = \frac{c_f max(m\left(t\right))}{\omega_{max}}$$

where ω_{max} is the maximum frequency content of the message signal and apply Carson's Rule for bandwidth estimation.

5.3 Noise Performance of classical FM

To evaluate the performance of FM modulation against channel noise we need models for both the receiver and the noise. We start with the receiver.

The receiver is a device that demodulates the FM signal to produce an output pro-

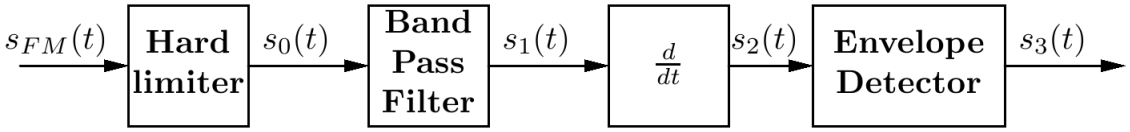

Figure 5.3: FM receiver

portional to the message signal. Such a device is also called a frequency discriminator which essentially works in 4 steps as shown in Figure 5.3 on page 41. First the hard limiter converts the received FM signal to a square wave $s_0(t)$ at the same frequency with constant amplitude to make receiver insensitive to amplitude variations. The square wave is then bandpass filtered at carrier frequency ω_c (and of bandwidth at least that of FM signal) to obtain again a sinusoidal waveform which will be ideally (without noise) of the form $s_1(t) = Acos\left(\omega_c t + c_f \int m(t)\, dt\right)$ for some amplitude A. This wave is then differentiated to get $s_2(t) = -A\left(\omega_c + c_f m(t)\right) sin\left(\omega_c t + c_f \int m(t)\, dt\right)$ and envelope detected to obtain an output $s_3(t) = A\left(\omega_c + c_f m(t)\right)$ proportional to $m(t)$.

The noise in communication channels is usually modeled as white Gaussian random process $N(t)$ with a constant spectral density function. But since the FM receiver described above has a bandpass filter stage, we will model the noise as a narrowband process $n(t)$ with frequency content of FM bandwidth $2\omega_m(1+\beta)$ centered around ω_c such that its spectral density is given by

$$S_n(\omega) = N_0/2 \tag{5.5}$$

for $\omega_c - (\Delta\omega + \omega_m) \leq |\omega| \leq \omega_c + (\Delta\omega + \omega_m)$ and zero otherwise. The narrowband noise process $n(t)$ can also be written in the form:

$$n(t) = \rho(t)\, cos\left(\omega_c t + \theta(t)\right) \tag{5.6}$$

where $\rho(t)$ and $\theta(t)$ are slowly varying amplitude and phase processes. Expanding Eq. 5.6:

$$\begin{aligned} n(t) &= \rho(t)\cos(\theta(t))\cos(\omega_c t) - \rho(t)\sin(\theta(t))\sin(\omega_c t) && (5.7)\\ &= n_i(t)\cos(\omega_c t) - n_q(t)\sin(\omega_c t) && (5.8) \end{aligned}$$

where $n_i(t)$ and $n_q(t)$ are in-phase and quadrature components of the narrowband noise respectively. It can be shown that the spectral density of the quadrature component is given by

$$S_{n_q}(\omega) = N_0 \tag{5.9}$$

for $|\omega| \leq (\Delta\omega + \omega_m)$. We will need this in the following SNR (signal to noise ratio) analysis.

We next assume that the transmitted FM signal is contaminated with the additive narrowband noise in the channel to produce the signal $r(t)$ at the input of the receiver:

$$\begin{aligned} r(t) &= s_{FM}(t) + n(t) && (5.10)\\ &= A_c cos\left(\omega_c t + c_f \int m(t)\,dt\right) + \rho(t)\cos(\omega_c t + \theta(t)) && (5.11)\\ &= A(t)\cos(\omega_c t + \phi(t)) && (5.12) \end{aligned}$$

where $A(t)$ won't have any role in our analysis due to hard limiter and the phase $\phi(t)$ is given by:

$$\phi(t) = c_f \int m(t)\,dt + arctan\left(\frac{\rho(t)\sin\left(\theta(t) - c_f\int m(t)\,dt\right)}{A_c + \rho(t)\cos\left(\theta(t) - c_f\int m(t)\,dt\right)}\right)$$

For the case of high carrier to noise ratio, $A_c \gg \rho(t)$, the phase $\phi(t)$ becomes approximately:

$$\phi(t) \backsimeq c_f \int m(t)\,dt + \frac{\rho(t)}{A_c} sin\left(\theta(t) - c_f \int m(t)\,dt\right) \tag{5.13}$$

We will neglect the message term in the argument of the sine function above. Its effect is to produce noise outside the message bandwidth which is irrelevant for our analysis [12]. Then Eq. (5.13) becomes:

$$\begin{aligned} \phi(t) &= c_f \int m(t)\,dt + \frac{\rho(t)}{A_c} sin\left(\theta(t)\right) && (5.14)\\ &= c_f \int m(t)\,dt + \frac{n_q(t)}{A_c} && (5.15) \end{aligned}$$

We have already said that amplitude of the received signal was irrelevant due to hard limiter in the receiver. We need to also determine the effect of later stages of the receiver on the phase in Eq. (5.15). For this we will assume that the differentiator and envelope detector stages correspond to differentiating the phase first and then lowpass filtering the result to the signal message bandwidth ω_m. Differentiating (5.15):

$$\frac{d}{dt}\phi(t) = c_f m(t) + \frac{1}{A_c}\frac{d}{dt} n_q(t) \tag{5.16}$$

Defining $n_o(t) = \frac{1}{A_c}\frac{d}{dt} n_q(t)$, we have:

$$\begin{aligned} S_{n_o}(\omega) &= \left|\frac{j\omega}{A_c}\right|^2 S_{n_q}(\omega) && (5.17)\\ &= \frac{\omega^2}{A_c^2} S_{n_q}(\omega) && (5.18) \end{aligned}$$

where $S_{n_q}(\omega)$ is the spectral density of the quadrature noise as defined in Eq. (5.9).

After lowpass filtering to the message bandwidth, noise spectral density becomes:

$$S_{n_o}(\omega) = \frac{\omega^2}{A_c^2} N_0 \tag{5.19}$$

for $|\omega| \leq \omega_m$. Now we can calculate total noise power $E\left\{n_o^2(t)\right\}$ at the output of the receiver:

$$E\left\{n_o^2(t)\right\} = \frac{1}{2\pi}\int_{-\omega_m}^{\omega_m} \frac{\omega^2 N_0}{A_c^2} d\omega \tag{5.20}$$

$$= \frac{\omega_m^2 N_0}{3\pi A_c^2} \tag{5.21}$$

The message power at the output is $c_f^2 \langle m^2(t)\rangle$ so that the output signal to noise ratio is:

$$SNR_0 = \frac{3\pi A_c^2 c_f^2 \langle m^2(t)\rangle}{\omega_m^3 N_0} \tag{5.22}$$

Signal power at the input of receiver is $A_c^2/2$ and the noise power at the input is computed using Eq. (5.5):

$$E\left\{n^2(t)\right\} = \frac{N_0(\Delta\omega + \omega_m)}{\pi} \tag{5.23}$$

The input signal to noise ratio is then:

$$SNR_i = \frac{\pi A_c^2}{2(\Delta\omega + \omega_m) N_0} \tag{5.24}$$

And the detection gain:

$$\frac{SNR_o}{SNR_i} = \frac{6c_f^2(\Delta\omega + \omega_m)\langle m^2(t)\rangle}{\omega_m^3} \tag{5.25}$$

For a single tone message signal $m(t) = A_m cos(\omega_m t)$ we have $\langle m^2(t) \rangle = A_m^2/2$ so that the detection gain is:

$$\frac{SNR_o}{SNR_i} = 3\beta^2(1+\beta) \tag{5.26}$$

So for a linear increase in bandwidth we obtain a noise reduction of the order of third power of the modulation index.

5.4 FM for protecting qubits during measurement

We model the FM modulator as a dynamical system consisting of two oscillators coupled in a nonlinear way. The hamiltonian of the system reads:

$$H_S = \frac{p_m^2}{2M_m} + \frac{1}{2}M_m\omega_m^2 x_m^2 + \frac{p_c^2}{2M_c} + \frac{1}{2}M_c(\omega_c + c_f x_m)^2 x_c^2 \tag{5.27}$$

Here x_m is the qubit degree of freedom to be protected (equivalent of message signal in classical FM) and x_c is the degree of freedom corresponding to the FM signal whose frequency is modulated by x_m around carrier frequency ω_c. We modeled the qubit part as an harmonic oscillator for the sake of simplicity and also to compare the noise performance with that of the classical FM which is usually analyzed assuming a single tone message signal. Also we don't expect the qubit hamiltonian to have an effect on the noise propagation from the FM part.

Imagine a typical operation of this system as follows: Noisy measurement devices will have access only to the FM signal x_c so that the qubit degree of freedom x_m will be protected from noise. Modeling the noisy environment as a bath of harmonic oscillators, the hamiltonian of the noisy system will read:

$$H = H_S + H_B + H_{SB} \tag{5.28}$$

where H_B and H_{SB} are given by:

$$H_B = \frac{1}{2}\sum_{\alpha}\left(\frac{p_\alpha^2}{m_\alpha} + m_\alpha\omega_\alpha^2 x_\alpha^2\right) \tag{5.29}$$

$$H_{SB} = x_c\sum_{\alpha} c_\alpha x_\alpha + \Delta U\left(x_c\right) \tag{5.30}$$

as in [8]. Classical equations of motion without bath reads:

$$\ddot{x}_m = -\omega_m^2 x_m - c_f\left(\frac{M_c}{M_m}\right)\left(\omega_c + c_f x_m\right)x_c^2 \tag{5.31}$$

$$\ddot{x}_c = -\left(\omega_c + c_f x_m\right)^2 x_c \tag{5.32}$$

In classical FM the frequency deviation $\Delta\omega = |c_f x_m|$ is usually assumed to be small compared to the carrier frequency ω_c , i.e. $\Delta\omega \ll \omega_c$. With this assumption, equations (5.31) and (5.32) can be written approximately:

$$\ddot{x}_m = -\omega_m^2 x_m - c_f\left(\frac{M_c}{M_m}\right)\omega_c x_c^2 \tag{5.33}$$

$$\ddot{x}_c = -\omega_c^2\left(1 + \frac{2c_f x_m}{\omega_c}\right)x_c \tag{5.34}$$

We won't try to solve those equations. We will rather assume that the solution of Eq. (5.34) is almost in FM signal form:

$$x_c\left(t\right) \simeq A_c cos\left(\omega_c t + c_f\int x_m dt\right) \tag{5.35}$$

and we will try to estimate the spectrum of the noise propagated to the qubit side. The assumption above is true if $\omega_m \ll \omega_c$ holds.

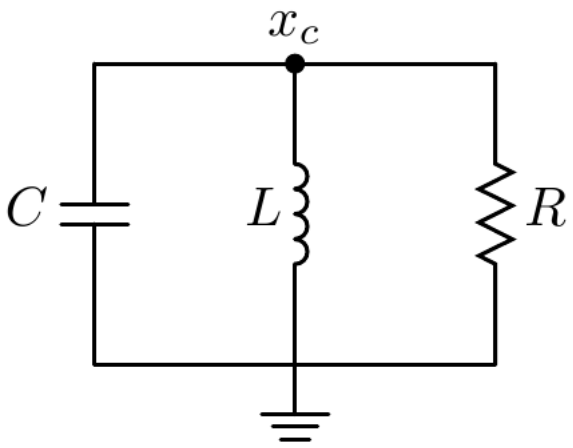

Figure 5.4: Equivalent circuit for the environment and FM signal

We note that noise will enter the qubit through the quadratic term x_c^2 in Eq. (5.33). Also due to this quadratic term, x_m will have a DC component and a component at $\omega = 2\omega_c$ which can be neglected compared to its natural frequency oscillations

$$x_m(t) \simeq A_m cos(\omega_m t) \tag{5.36}$$

If we linearize Eq. (5.33) around solutions in Eq. (5.36) and (5.35) we get:

$$\delta\ddot{x}_m = -\omega_m^2 \delta x_m - 2c_f \left(\frac{M_c}{M_m}\right) \omega_c A_c cos(\omega_c t)\, \delta x_c \tag{5.37}$$

where FM solution is further assumed to be $x_c(t) \simeq A_c cos(\omega_c t)$.

Now the variable δx_c corresponds to noise filtered by FM part. This noise corresponds to the fluctuations of the FM signal degree of freedom x_c. To find the spectrum of these fluctuations we will map the hamiltonian description of the FM signal bath coupling in Eqs. (5.28), (5.29), (5.30) to an equivalent parallel RLC circuit as in Figure 5.4 on page 47 and compute the spectrum with the fluctuation-dissipation theorem. Approximating FM part with an harmonic oscillator of frequency ω_c and mass M_c, we map to the circuit as follows:

$$\omega_c = \frac{1}{\sqrt{LC}} \tag{5.38}$$

$$Z_c = \sqrt{\frac{L}{C}} = \frac{1}{\omega_c M_c} \tag{5.39}$$

Now the real part of the impedance is:

$$Re\left[Z\left(\omega\right)\right] = Re\left[\frac{1}{j\omega C + \frac{1}{j\omega L} + R^{-1}}\right] \tag{5.40}$$

$$= \frac{Z_c^2 \omega_c^2 \omega^2 R^{-1}}{\left(\omega^2 - \omega_c^2\right)^2 + Z_c^2 \omega_c^2 \omega^2 R^{-2}} \tag{5.41}$$

and the spectrum of the fluctuations is given by the fluctuation-dissipation theorem:

$$S_{\delta x_c}\left(\omega\right) = \frac{\hbar}{\omega}\left[coth\left(\frac{\beta\hbar\omega}{2}\right) + 1\right] Re\left[Z\left(\omega\right)\right] \tag{5.42}$$

$$= \frac{\hbar Z_c^2 \omega_c^2 \omega R^{-1}}{\left(\omega^2 - \omega_c^2\right)^2 + Z_c^2 \omega_c^2 \omega^2 R^{-2}}\left[coth\left(\frac{\beta\hbar\omega}{2}\right) + 1\right] \tag{5.43}$$

$$= \frac{\hbar M_c^{-2} \omega R^{-1}}{\left(\omega^2 - \omega_c^2\right)^2 + M_c^{-2} \omega^2 R^{-2}}\left[coth\left(\frac{\beta\hbar\omega}{2}\right) + 1\right] \tag{5.44}$$

where $\beta = 1/k_B T$. $S_{\delta x_c}\left(\omega\right)$ has a Lorentzian shape peaked at ω_c .

If we define the random process in Eq. (5.37) as:

$$n\left(t\right) = 2c_f\left(\frac{M_c}{M_m}\right)\omega_c A_c cos\left(\omega_c t\right)\delta x_c\left(t\right) \tag{5.45}$$

then its spectrum is given by:

$$S_n\left(\omega\right) = c_f^2\left(\frac{M_c}{M_m}\right)^2 \omega_c^2 A_c^2\left[S_{\delta x_c}\left(\omega - \omega_c\right) + S_{\delta x_c}\left(\omega + \omega_c\right)\right] \tag{5.46}$$

Hence we see that the spectrum of the noise is filtered Eq. (5.41), scaled and shifted Eq. (5.46) before entering qubit equation Eq. (5.33). $S_n(\omega)$ is the effective spectrum seen by the qubit.

Assuming $\omega_m \ll \omega_c$ we see from Eq. (5.44) that the noise is filtered by a factor of $\frac{\omega_m}{\omega_c^4}$ at $\omega = \omega_m$. Taking the factors in front of Eq. (5.46) into account the noise power at $\omega = \omega_m$ before shifting is

$$\left(c_f^2 \left(\frac{M_c}{M_m} \right)^2 \omega_c^2 A_c^2 \right) S_{\delta x_c}(\omega_m) = c_f^2 \frac{A_c^2}{M_m^2} \frac{\omega_m}{\omega_c^2} \frac{1}{R} \tag{5.47}$$

Due to the shifting, $S_n(\omega)$ will have components peaked at DC and $\omega = 2\omega_c$. The component centered at DC seems problematic since it may increase the noise power $S_n(\omega)$ at $\omega = \omega_m$ which in turn will increase relaxation rate of the qubit. More importantly however, the increase in DC noise power will increase the dephasing rate.

Now this noise power appearing at DC make me doubt about the performance of the FM system I proposed above. I wonder if such a system would improve noise performance compared to a simple bandpass filter placed between the qubit and the measurement device.

However one should not be too pessimistic since the analysis above is in the zeroth order considering the bandwidth of an FM signal modulated by a sinusoidal message signal. Such an FM signal has bandwidth given by Bessel functions of the first kind and the component centered at ω_c can be made to vanish by a suitable choice of the modulation index β. Hence one may get rid of the DC noise which induce dephasing.

Chapter 6

CONCLUSION

In this thesis we have reviewed methods to derive hamiltonians for lumped element superconducting circuits. We also looked at the quantization of transmission lines. We then reviewed basic superconducting qubits. In Chapter 4 we analyzed a couple of schemes for the tunable coupling of qubits to transmission lines. Superconducting circuits are easy to control but they couple to the environment stronger compared to microscopic qubit implementations which increase their decoherence rates.

In Chapter 5 we proposed a new scheme to protect qubits during measurement. If the measurement process is relatively long (continuous type of measurement), one would require the decoherence time of the qubit to be long enough so that the measurement will be completed before the qubit decoheres. In such a situation it might be better to first frequency modulate the qubit degree of freedom and let the noisy measurement device have only access to the FM signal. This way one may hope the noise propagated to the qubit side to be suppressed remembering the good noise performance of classical FM.

We devised a mathematical model for such an FM system and made a preliminary noise analysis.

We note that the FM system we proposed in Chapter 5 is only mathematical. Implementing it in superconducting circuits is another problem. One should also analyze how the FM modulated signal would effect the measurement rate and fidelity considering the additional demodulation stage that would be needed in the measurement device. One can also consider coupling control devices to the FM part instead of coupling them directly to the qubit.

Chapter 7

APPENDIX

DC SQUID

Circuit diagram of the DC SQUID is presented in Figure 7.1 on page 52. DC SQUID consists of a loop with two Josephson junctions biased by an external flux Φ_x. We neglect inductances of each loop branch for the sake of simplicity. We also assume that the junctions are identical so that the Josephson energies are equal $E_{J1} = E_{J2} = E_J$. In this case the critical current of each junction is equal and given by $I_{c1} = I_{c2} = I_c = 2\pi E_J/\Phi_0$. Denoting phase drops across each junction by φ_1 and φ_2 we write the Kirchhoff's voltage law around the loop as $\varphi_1 - \varphi_2 + f = 0$, where $f = 2\pi\frac{\Phi_x}{\Phi_0}$. We now write Kirchhoff's current law at node a:

$$
\begin{aligned}
I &= I_1 + I_2 && (7.1)\\
&= I_{c1} sin\,(\varphi_1) + I_{c2} sin\,(\varphi_2) && (7.2)\\
&= I_c sin\,(\varphi_1) + I_c sin\,(\varphi_1 + f) && (7.3)\\
&= I_c sin\,(f)\, cos\,(\varphi_1) + I_c\,(1 + cos\,(f))\, sin\,(\varphi_1) && (7.4)\\
&= I_c^{'} sin\,(\phi) && (7.5)
\end{aligned}
$$

where

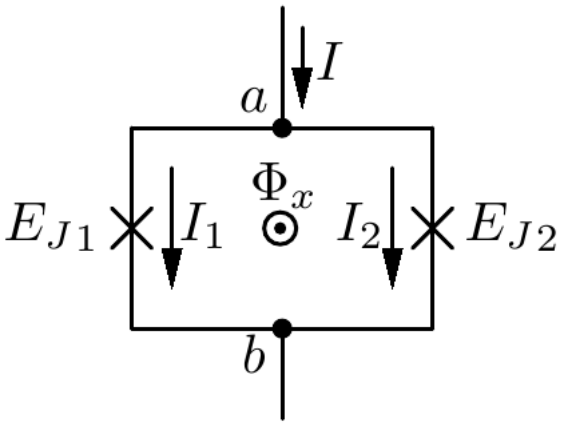

Figure 7.1: DC SQUID circuit

$$I_c^{'} = I_c\sqrt{\left[sin^2\left(f\right)+\left(1+cos\left(f\right)\right)^2\right]} \tag{7.6}$$

$$= I_c\sqrt{2+2cos\left(f\right)} \tag{7.7}$$

$$= 2I_c cos\left(f/2\right) \tag{7.8}$$

and $\phi = \varphi_1 + \eta$ with $\eta = f/2$.

So we see that the DC SQUID behaves effectively like a single junction of critical current $I_c^{'} = 2I_c cos\left(f/2\right)$, effective Josephson energy $E_J^{'} = 2E_J cos\left(f/2\right)$ and phase $\phi = \varphi_1 + f/2 = \varphi_2 - f/2$ satisfying the Josephson current relation:

$$I = I_c^{'} sin\left(\phi\right) \tag{7.9}$$

BIBLIOGRAPHY

[1] A. O. Caldeira and A. J. Leggett, Ann. Phys. (N. Y.) 143, 374 (1983)

[2] Michel Devoret, Lectures on mesoscopic physics, College de France, http://www.physinfo.fr/lectures.html

[3] M. H. Devoret, Quantum Fluctuations (Les Houches Session LXIII), Elsevier 1997, pp. 351–386.

[4] Audrey Cottet, Implementation of a quantum bit in a superconducting circuit, PhD thesis, Université Paris VI, 2002.

[5] T. P. Orlando, J. E. Mooij, L. Tian, C. H. van der Wal, L. S. Levitov, S. Lloyd, J. J. Mazo, Phys. Rev. B 60, 15398 (1999)

[6] John S. Denker, Capacitance, http://www.av8n.com/physics/capacitance.htm

[7] B. Peropadre, P. Forn-Díaz, E. Solano, and J. J. García-Ripoll, PRL 105, 023601 (2010)

[8] G. Burkard, R. H. Koch, and D. P. DiVincenzo, "Multi-level quantum description of decoherence in superconducting flux qubits," Phys. Rev. B 69, 064503 (2004); cond-mat/0308025

[9] Yu. Makhlin, G. Schön, and A. Shnirman, Quantum-state engineering with Josephson-junction devices, Rev. Mod. Phys. 73, 357-400 (2001)

[10] B. Yurke and J. S. Denker, "Quantum network theory," Physical Review A, 29 [3] 1419-1437 (1984).

[11] K. K. Likharev, Dynamics of Josephson Junctions and Circuits (Gordon and Breach, New York, 1986)

[12] Jerry D. Gibson, Principles of Digital and Analog Communications, (Macmillan Publishing Company, 1993)

[13] Callen H. B. and T. A. Welton, 1951, Phys. Rev. 83, 34

[14] Lin Tian, Seth Lloyd, T. P. Orlando, Phys. Rev. B 65, 144516 (2002)